Photon Lasers Med 1 (2012): 123–131 © 2012 by Walter de Gruyter • Berlin • Boston. DOI 10.1515/plm-2012-0007

Near infrared *ex-vivo* bovine and computer model thresholds for laser-induced retinal damage

Rinder *Ex-vivo*- und Computermodell-Schwellwerte für die laser-induzierte Schädigung der Netzhaut im nahen infraroten Wellenlängenbereich

Karl Schulmeister*, Rahat Ullah and Mathieu Jean

Laser Safety Test House and Consulting, Seibersdorf Labor GmbH, A-2444 Seibersdorf, Austria,
e-mail: karl.schulmeister@seibersdorf-laboratories.at

* Corresponding author

Abstract

Thresholds for thermal damage of the retina were determined with excised bovine eyes and a computer model for 1090 nm laser radiation in the applicable pulse duration regime and for varying retinal laser spot diameters. The thresholds compare well with available rhesus monkey data, further validating the models for absolute threshold predictions and parameter studies including in the near infrared (NIR) range up to about 1340 nm. The variation of the spot size dependence for different pulse durations that was found in an earlier study for the wavelength of 532 nm was confirmed, which supports the proposed amendment of ICNIRP, ANSI and IEC laser and incoherent optical radiation exposure limits. The earlier conclusion that the damage mechanism at threshold determined 24 h and 1 h after exposure for the non-human primate (NHP) model is retinal pigment epithelium (RPE) cell damage and not thermal coagulation of the sensory retina was confirmed. The data in the NIR range indicate that scattering within the RPE and choroid does not significantly enlarge the effective spot size, and that the rhesus monkey minimal spot *in vivo* threshold in that wavelength range can be modeled best by assuming a spot diameter of 90 μm, supporting an earlier suggestions that pre-RPE scattering leads to an enlargement of the retinal spot size for NHP *in-vivo* studies. Following the validation with rhesus monkey and bovine data, also for the NIR range, the computer model can be used to study threshold dependencies as well as for hazard analysis for exposure in the pulse duration range applicable for thermally induced injury. This is particularly relevant for irregular pulse patterns or scanned retinal exposure, where the current laser safety standards do not provide specific methods, leading to over-restrictive results.

Keywords: laser safety; retinal thermal injury;damage threshold; computer model; IEC 60825-1; ANSI Z136.1.

Zusammenfassung

Die vorliegende Arbeit dokumentiert Schwellwerte für die thermisch induzierte Schädigung der Netzhaut für eine Laserwellenlänge von 1090 nm, die am *Ex-vivo*-Modell (Rind) und mit Hilfe eines Computermodells für den anwendbaren Pulsdauer- und Fleckgrößenbereich ermittelt wurden. Dieser Datensatz ergänzt Schwellwerte für die Laserwellenlänge von 532 nm aus früheren Studien an Rhesusaffen und dem Rindermodell. Die ermittelten Schwellwerte passen gut mit den verfügbaren experimentellen Schwellwerten von Rhesusaffen zusammen, woraus geschlossen werden kann, dass die beschriebenen Modelle für Expositionsdauern zwischen 100 μs und mehreren Sekunden für alle Spotgrößen gültige Methoden darstellen, um Schwellwerte von Affen und Menschen auch im nahen Infrarotbereich (bis zu einer Wellenlänge von ca. 1340 nm) vorauszusagen. Die vorgeschlagene Änderung der internationalen Grenzwerte für gepulst emittierende ausgedehnte Quellen, für die ein pulsdauerabhängiger kritischer Winkel α_{max} definiert wurde, konnte hiermit für den gesamten relevanten Wellenlängenbereich validiert werden. Die Daten lassen den Schluss zu, dass im nahen Infrarotbereich Streuung innerhalb des retinalen Pigmentepithels (RPE) kein relevanter Effekt ist und sie sind mit der Annahme eines minimalen Laserflecks auf dem RPE von 90 μm Durchmesser konsistent, wobei pre-RPE-Streuung als Grund für die Vergrößerung des Spots vermutet wird. Auch wird die frühere Schlussfolgerung gefestigt, dass der primäre Schädigungsmechanismus für die 1 h oder 24 h nach Exposition festgestellten Schädigungsschwellwerte im Rhesusaffen-Modell eine unmittelbare RPE-Zellschädigung und keine Koagulation der Photorezeptoren darstellt. Da das Computermodell mit *In-vivo*-Schwellwerten vom Rhesusaffen und *Ex-vivo*-Schwellwerten vom Rind sowohl im sichtbaren wie auch im nahen infraroten Wellenlängenbereich validiert wurde, können künftig Untersuchungen zu Abhängigkeiten von Einflussgrößen und Sicherheitsanalysen im entsprechenden Pulsdauer- und Wellenlängenbereich auch mit dem Computermodell durchgeführt werden. Dies ist besonders für unregelmäßige Pulsfolgen oder eine gescannte Bestrahlung der Netzhaut relevant, wo die derzeitigen Lasersicherheitsnormen unvollständige oder überrestriktive Evaluierungsmethoden spezifizieren.

Schlüsselwörter: Lasersicherheit; thermische Schädigung; Netzhaut; Schwellwert; Computermodell; EN 60825-1.

1. Introduction

Intense optical radiation, particularly laser radiation, can induce temperatures in the retina that cause permanent damage. The exposure level that results in a minimally visible lesion, i.e., the threshold for injury, depends on wavelength, pulse (exposure) duration, and retinal image diameter [1, 2]. In a previous study [3], we have presented *ex-vivo* and computer model threshold data for the wavelength of 532 nm that, for the first time, fully characterized the dependence of the retinal injury threshold on retinal image (spot) diameter for the relevant range of pulse durations. Here we present *ex-vivo* and computer model data obtained with a wavelength of 1090 nm that complements the set of thresholds determined for the visible (VIS) wavelength range. These data provide the basis for improving the accuracy of the laser, as well as the broadband optical radiation exposure limits for extended apparent sources and pulsed exposures, by introducing a pulse duration dependent critical angular subtense of the apparent source α_{max}, as proposed by Schulmeister et al. [4]. International laser exposure limit guidelines published by the International Commission on Non-Ionizing Radiation Protection (ICNIRP) [5], national standards such as ANSI Z136.1 in the US [6] and the laser product safety standard IEC 60825-1 [7] are currently under revision and committee draft documents feature the corresponding improved limits that will raise the permitted exposure level for laser radiation by up to a factor of 20. Exposure limit guidelines for optical broadband radiation as developed by ICNIRP [8] as well as light emitting diode (LED) and lamp product safety standards [9, 10] are also to be amended, providing for harmonization between laser and broadband optical radiation retinal thermal exposure limits [11].

We present retinal injury threshold data both in terms of the intraocular energy (IOE), and in terms of retinal radiant exposure; for a more detailed discussion on the definition, corresponding transformation and on presenting retinal injury data and exposure limits as function of retinal spot size, see [3] or [4].

2. Materials and methods

2.1. Experimental procedure

The schematic overview of the experimental setup is shown in Figure 1. A fiber laser (SP-120C; SPI Lasers, Southampton, UK) emitting at a wavelength of 1090 nm with a maximal output power of 120 W was used to expose harvested bovine samples. The laser output power as well as the pulse duration (rectangular temporal profile, pulse duration between 1 ms and 1 s) was controlled with a personal computer (PC). The beam profile was Gaussian with a beam propagation factor M^2 of 1.08. Two wedges were used to reduce the beam power to the range needed for exposure, since the computer control of the laser power did not have sufficient resolution and the laser output was not stable for power levels below 700 mW. A combination of lenses was used to achieve the desired beam diameter on the sample. A galvanometer-driven scanner (hurry SCAN® II 14; SCANLAB, Puchheim, Germany) produced a user-defined exposure pattern on the sample. A PC interface card (RTC®4; SCANLAB, Puchheim, Germany) and self-developed software was used to control the scanner (the position of the beam on the sample), the laser pulse duration, as well as the laser output power. This automated exposure system makes it possible to expose a sample with a grid of individual laser exposures for a given pulse duration and spot size with varying peak power in a short period of time. Before exposure, the laser power was measured at each location, at or near the sample position, using a calibrated laser power meter [model 3A and L40(150)A; Ophir Optronics Ltd., North Logan, UT, USA]. Also before each exposure series, the spatial beam profile in the sample plane was measured with a charge-coupled device (CCD) camera (model 7512; Cohu, Inc., San Diego, CA, USA) with 6.7-µm pixel pitch, and the beam diameter defined at the 1/e irradiance level was calculated with a beam analyzer software (Spiricon LBA-700PC; Ophir Optronics Ltd., North Logan, UT, USA). The beam profile at the position of the sample was Gaussian for all spot sizes.

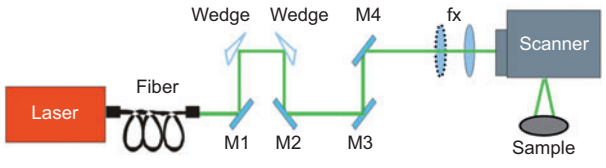

Figure 1 Experimental set-up for the *ex-vivo* sample exposures.

2.2. Tissue model

The *ex-vivo* (explant) samples were obtained from fresh bovine eyes which were received from a local slaughterhouse. Porcine eyes, which would be a model without a tapetum lucidum, were not available, as animals were immersed in boiling water immediately after slaughter. The bovine eyes were dissected and for the posterior hemisphere, the vitreous and sensory retina removed, so that the retinal pigment epithelium (RPE) was the uppermost layer (only sections outside of the tapetum lucidum were used, which is about half of the available area). The sample preparation and threshold determination was identical to the one used in the earlier 532 nm series [3]. As in the previous study, the tissue was stained with the marker Calcein AM and following laser exposure, cell viability as indicated by fluorescence was visually determined with a microscope (Figure 2). The lesion dose-response data was evaluated by a Probit analysis software (ProbitFit V1.0.2 by Brian Lund, US Army Institute of Surgical Research, San Antonio, TX, USA) to obtain effective dose 50 (ED50) and slope values (see for instance Sliney et al. [12] for a discussion on these parameters).

2.3. Computer model

A computer model was developed and validated against the complete data set of applicable non-human primate (NHP) threshold data for thermally induced retinal injury [13].

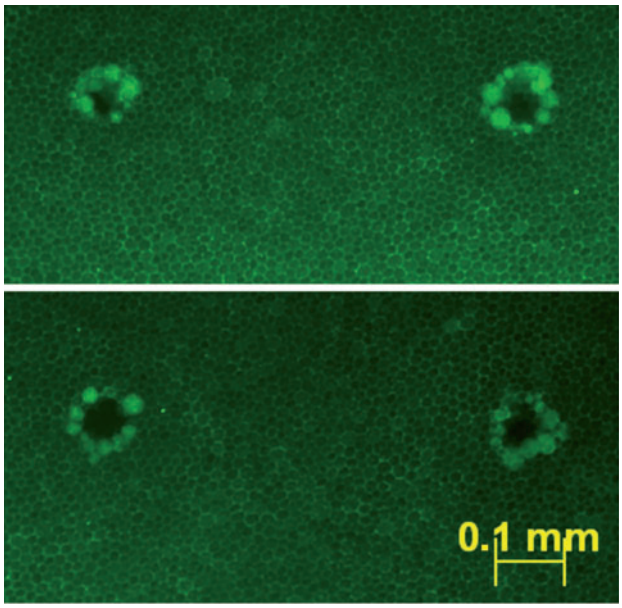

Figure 2 Fluorescent micrograph of exposures with a beam diameter of 80 µm and a pulse duration of 1 ms. Individual viable RPE cells are visible, dead cells appear dark.

The model can be considered as standard and has been applied to model laser-induced injury thresholds since the 1970s [14]. The two-dimensional heat flow equation (using axial symmetry) was solved numerically with a commercial finite element package (COMSOL Multiphysics® V.3.2.; COMSOL AB, Stockholm, Sweden) to obtain the temperature as function of time, and the Arrhenius integral [15] was used to determine injury thresholds. A slab geometry was assumed. The thermal properties of all media were taken as that of water at a temperature of 40°C. The Beer-Lambert's law of absorption was used for all layers. The laser peak power was adjusted so that within the RPE, the Arrhenius integral reached a value of 1 on the edge of a circle of 50 µm in diameter. This diameter can be considered equivalent to a minimum visible lesion (MVL) diameter for the NHP threshold studies. Threshold determination in the computer model was variable in terms of depth, i.e., the full RPE was "scanned" to identify the position where the threshold was reached with the lowest power. The NHP model distinguishes between exposures in the macula (with a denser pigmentation) and exposures in the paramacula, while the experimental NHP threshold data set was not consistent enough to differentiate the computer model into 1 h and 24 h endpoints of observation of damage after the exposure. The NHP model was also used to model the bovine thresholds, i.e., the Arrhenius damage integral, layer thicknesses and thermal property parameters were the same. For the bovine computer model, the absorption data for NHP paramacular sites was used and the tissue background temperature was changed from 37°C for the NHP model to 24°C for the bovine model. For the NHP model it was necessary to assume a minimum spot size of 90 µm at 1/e irradiance levels for a wavelength of 1090 nm in order to properly model minimal spot size thresholds, as will be discussed below. The model parameters are given in Tables 1 and 2.

3. Results

The bovine *ex-vivo* damage thresholds (i.e., ED50) are summarized in Table 3. The overall variability and uncertainty of the ED50 values is estimated to be about ±20%. The *ex-vivo* thresholds cover a pulse duration range of 1 ms to 1 s and a spot diameter range (1/e irradiance levels) of 26 µm to 2.5 mm. The slope S (ED84/ED50) that results from Probit analysis of the experimental data is mostly between 1.1 and 1.25, indicating little variability within one sample and between different eyes, as well as a relatively small uncertainty. When the slope is listed as <1.01, the Probit analysis software indicated that positive and negative responses did not overlap (i.e., basically a step function) and the value of the slope was so close to 1 that the calculated slope (<1.01) was uncertain. To derive the 17 threshold injury values, a total number of 3453 exposures were placed on 184 samples.

As for the 532 nm wavelength study, the bovine *ex-vivo* model and the computer model can be validated by comparison with rhesus monkey *in-vitro* threshold data. Rhesus monkey data that is available in the respective pulse duration regime for laser wavelengths close to 1090 nm is summarized in Table 4. Only two thresholds were identified for this parameter range which were obtained for a defined retinal spot size. Vincelette et al. [16] determined the threshold for a spot size of 100 µm at 1/e irradiance levels for a pulse duration of 100 ms, while Ham et al. [17] reported a threshold for a pulse duration of 1 s for a retinal 1/e spot size of 275 µm (the value given by Ham et al. was corrected to account for the nominal focal length of the relaxed rhesus monkey of 13.5 mm instead of the 17 mm used by Ham et al.). The studies by Skeen et al. [18] and Vassiliadis et al. [19] provide thresholds for a range of pulse durations for what could be called minimal spot conditions, i.e., a collimated laser beam, where the actual retinal spot diameter is not characterized. The Skeen study [18] extends over a larger pulse duration range and data is obtained for macular sites only, while the thresholds by Vassiliadis et al. [19] were obtained for pooled data from both

Table 1 General model parameters for the computer model used to predict damage thresholds, optimized and validated for relevant NHP threshold data [13]. Adaptations for the bovine computer model are listed where applicable.

	Parameter	Unit	Value
Thermal properties	Conductivity	W/(m·K)	0.635
	Specific heat	J/(kg·K)	4178
	Density	kg/m^3	992
	Body temperature	K	310 (NHP), 297 (bovine)
Damage model	MVL diameter	µm	50 (NHP), 30 (bovine)
	Pre-exponential factor	1/s	8×10^{98}
	Inactivation energy	K	75,000

Table 2 Layer-specific model parameters for the computer model used to predict damage thresholds, optimized and validated for relevant NHP threshold data [13]. Adaptations for the bovine computer model are listed where applicable.

Layer	Thickness (μm)	Pigmentation	Absorption coefficient (cm^{-1})	Reflection at front (%)
RPE (paramacula)	6	100% ME	$3.85\times10^{14}\ \lambda^{-4.2}$	1.7
Pigment-free intermediate layer	4	–	–	–
Choroid	170	70% ME; 30% BL	$e^{-0.004\ \lambda+6.75}$	–
Sclera	∞	–	–	$100\text{-}67\times\exp[-3\times10^{-6}\ (\lambda\text{-}660)^2]$

ME, melanin; BL, blood (oxyhemoglobin); λ, wavelength in the unit of nm.

Table 3 Probit threshold data for the range of pulse durations between 1 ms and 1 s and retinal spot diameters, where relevant, from 26 μm to 2.5 mm for the bovine *ex-vivo* explant model for 1090 nm laser radiation. The slope *S* is defined as ED84/ED16. The profile for all retinal spots was Gaussian (1/e diameter criteria). The ED50 given as radiant exposure was determined from the ED50 given in terms of energy divided by the area calculated from the spot diameter.

Pulse duration (ms)	Spot diameter (μm)	ED50 (mJ)	ED50 (J/cm^2)	Lower FL (J/cm^2)	Upper FL (J/cm^2)	Slope S	Number of samples	Number of exposures
1	26	0.156	29.43	27.76	30.99	1.17	11	239
	80	0.503	10.01	9.37	10.61	1.09	6	96
	261	3.05	5.701	5.25	6.07	1.25	12	206
	1120	49.2	4.99	4.72	526	1.2	32	128
10	26	1.0	188.9	181.0	196.6	1.21	11	363
	80	1.54	30.57	29.39	31.69	1.15	5	245
	261	5.70	10.65	9.81	11.44	1.17	4	100
	1120	111.3	11.30	9.53	12.69	1.22	13	52
100	26	6.06	1142	1075	1206	1.25	10	250
	80	9.14	181.8	176.8	186.6	1.15	9	288
	261	21.3	39.79	38.48	41.12	1.18	9	324
	1120	222.4	22.57	21.53	23.57	1.10	9	81
1000	26	39.9	7523	7211	7808	1.16	8	228
	80	66.1	1315	1251	1380	1.28	13	421
	261	154.8	289.3	281.9	296.9	1.14	12	352
	1120	636.8	64.64	60.74	67.09	1.09	16	64
	2539	2250	44.47	44.47	44.47	<1.01	4	16

FL, fiducial limits.

Table 4 Available experimental NHP threshold data in the wavelength range of 1060–1100 nm and pulse durations between 100 μs and 1 s. The IOE is the basic threshold information (directly measured), the retinal radiant exposure is calculated according the assumed retinal spot diameter (1/e irradiance points) and ocular transmission (0.62).

Reference	Wavelength (nm)	Endpoint	Pulse duration (ms)	Nominal spot diameter (μm)	ED50/IOE (mJ)	Calculated retinal radiant exposure (J/cm^2)
Vincelette et al. [16]	1110	24 h after exposure, paramacula	100	100	19.3	
Ham et al. [17]	1064	24 h after exposure, paramacula	1000	275	145	151.39
Skeen et al. [18]	1060	1 h after exposure, macula	1	90	0.44	38.59
			10	90	1.4	122.80
			100	90	6.7	587.67
			1000	90	43	3771.62
Vassiliadis et al. [19]	1060	1 h after exposure, paramacula and macula mixed	10	90	1.75	153.50
			100	90	9.6	842.04
			1000	90	53.8	4715.40

macular and paramacular exposure sites. Another difference is that Vassiliadis et al. [19] used a lens to compensate for chromatic aberration (which should in principle result in a smaller spot size and lower threshold when expressed as IOE), Skeen et al. [18] did not correct for chromatic aberration. It is noted that the thresholds reported by Skeen et al. [18] are consistently lower than the ones by Vassiliadis et al. [19] by a factor of 1.25–1.43, indicating that the retinal location has a larger effect than correcting for chromatic aberration. We have used the Skeen data for the validation of our NHP computer model

(which distinguished between macular and paramacular exposure), and account for the chromatic aberration (together with a minimal lesion diameter of 50 µm) by assuming a minimal spot size of 90 µm. The ratio of the predictions of the NHP computer model to the rhesus monkey data by Skeen et al. [18] lies between 1.01 and 1.1, i.e., a difference of not more than 10%.

The *ex-vivo* threshold data, the results of the NHP and bovine computer model as well as the *in-vivo* NHP threshold data are plotted in Figure 3 as function of pulse duration and in Figure 4 as function of retinal spot diameter. The data is expressed in Figures 3A and 4A in terms of retinal radiant exposure, obtained by dividing the thresholds expressed as energy per pulse by the area that corresponds to the 1/e diameter value. The NHP thresholds (experimentally determined as IOE) were corrected with a pre-retinal transmission factor of 0.62 [20] to calculate retinal levels. For Figures 3B and 4B, where the data is plotted in terms of IOE, the bovine *ex-vivo* thresholds were increased correspondingly by a factor of 1/0.62 to calculate thresholds levels that would apply if the *ex-vivo* bovine RPE were placed in a rhesus monkey eye. The bovine computer model and the NHP computer model fit the respective experimental threshold data well for the full pulse duration and spot size range, with a maximum deviation of 0.80–1.57 and 0.85–1.12 for the *ex-vivo* bovine and *in-vitro* NHP data, respectively (the ratio of computer model to NHP threshold for the case of the 1110 nm threshold refers to the computer model predictions for that wavelength; the plotted model data are for 1060 nm, which are correspondingly lower).

There is some uncertainty regarding the diameter of the retinal irradiance profile for the NHP data, as it cannot be measured directly. The assumed or inferred retinal spot size strongly affects the value of the threshold when expressed as retinal radiant exposure, and when plotted as function of spot size affects the position on the abscissa. It is only for the plot of the IOE as function of pulse duration where the (assumed) spot size has no direct effect (Figure 3A), and thus this presentation is the most relevant for comparing NHP and bovine data. For the long pulse duration regime, for all spot sizes, the trend of the data follows a $t^{0.8}$ dependence, which is somewhat steeper than the exposure limit dependence of $t^{0.75}$, and similar to the trend found for the wavelength of 532 nm. For shorter pulse durations, the pulse duration dependence becomes shallower; the pulse duration where this occurs shifts from short pulse durations (1–10 ms) for the small spot case to longer pulse durations (0.1–1 s) for larger spots. For pulse durations below about 0.1 ms, the calculated thermal injury thresholds approach the thermal confinement regime where there is no predicted pulse duration dependence. However, it should be noted that for pulse durations of the order of 10 µs or shorter, the thermal model is no longer applicable, as local melanosome heating leads to micro-cavitation induced cell death at lower radiant exposures than are necessary to induce thermal injury [4].

To be able to study the trends in the minimal spot regime (where complete NHP data sets are available) in more detail, we have plotted the data for the smallest spots in Figure 3C normalized to the 26 µm bovine computer model data. The comparison of the "minimum spot" NHP data with the bovine data plotted in Figure 3B,C shows that for 1 s pulse duration,

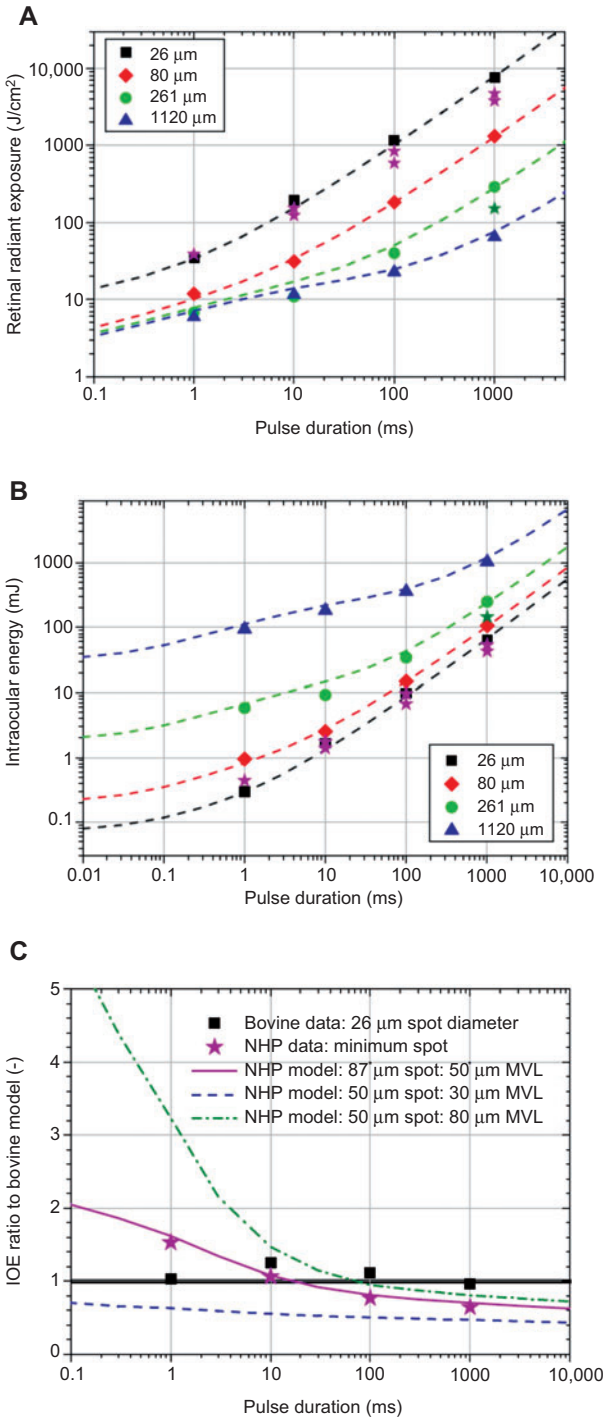

Figure 3 Damage threshold values for *ex-vivo* bovine samples, NHP thresholds (star symbols) and computer models as function of pulse duration and plotted as (A) retinal radiant exposure and (B) IOE. To transfer data from the corneal (IOE) to the retinal level or vice versa, a pre-retinal transmittance of 0.62 was assumed. In (C) data for the minimal spot region are plotted relative to the 26 µm bovine computer model data, which is shown as a line with value 1.

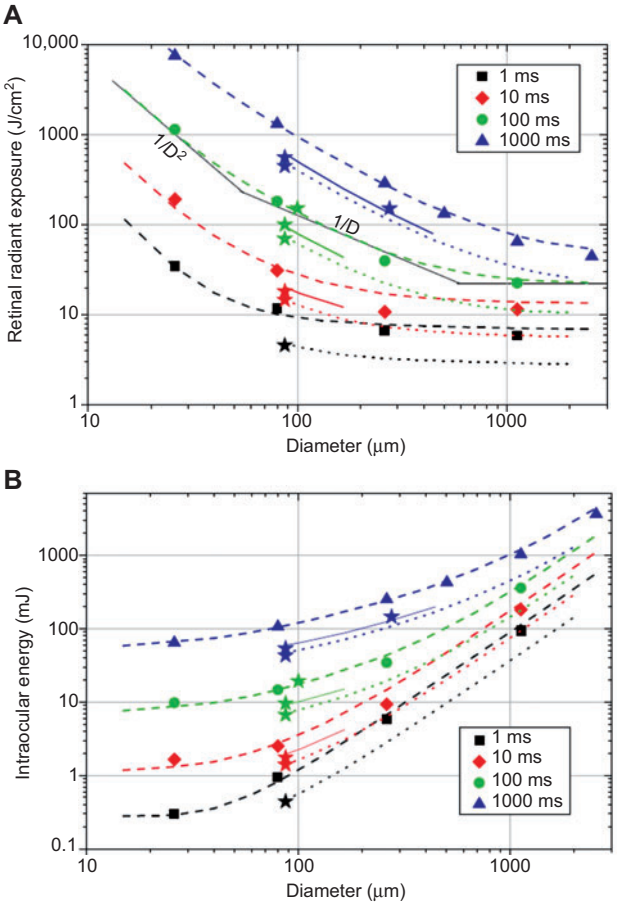

Figure 4 The threshold data that is shown in Figure 3, but as function of retinal laser spot diameter and plotted as (A) retinal radiant exposure and (B) IOE. For a given pulse duration, the NHP thresholds are lower than the corresponding bovine thresholds. Additionally to the bovine computer models (dashed lines), predictions of the NHP computer model are shown: dotted lines for macular exposure sites, thin full lines for paramacular exposure sites.

the NHP threshold is lower than the 26 µm bovine threshold, while for 1 ms, the NHP is somewhat higher than the corresponding 26 µm bovine threshold, i.e., the pulse duration dependence of the NHP thresholds is shallower than that of the 26 µm bovine data. The trend of the minimum spot NHP data shown in Figure 3B is similar (close to parallel) to the trend of the 80 µm bovine data, but the NHP thresholds are significantly lower. Both the NHP and the bovine experimental data sets can be modeled well when the retinal spot size is assumed to be 90 µm for the NHP model, and the nominal spot size is used for the bovine model, which is consistent with the visually observed trend of the minimal spot NHP thresholds being parallel to the 80 µm bovine data. The lower NHP thresholds as compared to the 80 µm bovine thresholds are modeled by accounting for the higher tissue temperature in the rhesus monkey and the higher pigmentation in the rhesus monkey macula (for the bovine model, the absorption parameters for rhesus monkey paramacular exposure are used). It is noted that the NHP thresholds calculated for an assumed spot size of 50 µm and a model-MVL of 80 µm shown in Figure 3C are significantly higher than the experimentally observed NHP threshold for the minimum spot condition.

Figure 4 shows the data in terms of spot size dependence. The minimal spot NHP data are plotted for an assumed spot diameter of 90 µm. The presentation as spot size dependence supports the choice of computer model parameters and assumed minimal spot size for the NHP data with a general good fit considering the wide range of pulse durations and spot sizes. The spot size dependence of the threshold data when expressed as retinal radiant exposure exhibits the same trend as seen for the wavelength of 532 nm: in the small diameter regime, the thresholds decrease for increasing diameters, in the large diameter regime, the thresholds do not depend on spot diameter. The transition region between these two regimes shifts from small diameters for short pulses to larger diameters for longer pulses. The dependence on spot diameter D is close to a $1/D^2$ trend for the small diameter section as indicated in Figure 4A with a thin line for the 100 ms data set (which when plotted as IOE, Figure 4B, appears as a region of no or little dependence on diameter). Between the small spot section and the range where there is no spot size dependence, the trend is similar to a $1/D$ dependence.

4. Discussion

4.1. Injury mechanism

Considering the wide range of pulse durations and retinal spot sizes, as well as different experimental conditions and endpoints, the differences between the *ex-vivo* bovine and the *in-vitro* NHP threshold data can be considered as surprisingly small. Furthermore, the differences between NHP and bovine thresholds can be explained well with the help of the computer model: once the *ex-vivo* sample temperature of 24°C vs. the NHP body temperature of 37°C, as well as the higher pigmentation of the NHP macula is considered, the largest deviation of respective model vs. experimentally obtained threshold is a factor of 1.6. Since thermally induced cell death at the RPE level is the background of the computer model (determined for the bovine model within minutes after exposure), the study further supports the conclusion of the 532 nm study [3] that the damage mechanism at threshold level for ophthalmoscopically minimal lesions detected *in vivo* at 1 h and 24 h after exposure is immediate thermally induced RPE cell death, not coagulation of the photoreceptors. This also strengthens the earlier validation of the bovine model as well as the computer model for thermally induce retinal injury and extends the validation into the near infrared (NIR) wavelength range. Both models should be applicable up to the wavelength range of about 1340 nm where the pre-retinal ocular media start to absorb considerably, potentially leading to thermal blooming [16], which cannot be modeled by the present bovine and computer model.

4.2. Minimum laser spot issue

Besides conclusions on the underlying injury mechanism, the comparison of thresholds from the different models also

provides information regarding the "minimum spot" issue (as discussed in the 532 nm study [3]), since the bovine model has the advantage that the retinal spot diameter can be determined directly with corresponding accuracy. The comparison of the pulse duration dependence of the bovine data with NHP thresholds plotted as IOE (Figure 3B,C) supports the conclusion that the NHP thresholds are consistent with a minimal retinal spot size in the range of 80–90 µm. For the case of the wavelength of 1060 nm, this cannot be explained by chromatic aberration alone, which would be in the range of 50 µm when given as 1/e diameter [16]. Also scattering within the RPE and choroid does not appear to lead to a significant increase of the effective retinal spot diameter that would affect injury thresholds. The IOE bovine threshold for a pulse duration of 1 ms and a spot size of 26 µm is a factor of 3.2 lower than the threshold for an 80 µm spot. If scattering were significant, the 26 µm threshold would be higher, closer to the threshold of the 80 µm spot. Also the bovine computer model – which uses the experimental laser spot diameter as model parameter – is consistent with that conclusion. In order to test the hypothesis that the higher NHP thresholds are not due to an enlarged laser spot diameter but are due to difficulties in observing small lesions, we have calculated NHP thresholds for a laser spot size of 50 µm and an MVL diameter of 80 µm, shown in Figure 3C relative to the bovine computer model thresholds for 26 µm spot size. These thresholds can be considered super-threshold, since the lesion, according to the hypothesis, has to be increased in visibility beyond the lesion at threshold (which is not visually discernible). The computer model predicts that the exposure levels necessary to produce a corresponding lesion in the RPE level are significantly higher than the experimentally observed ones (for information, we also plotted the predicted thresholds for a MVL diameter of 30 µm, which are correspondingly lower). This provides an additional argument that in the NHP experiments scattering, either within the nerve fiber layers or in anterior ocular media, results in an enlargement of the laser spot incident on the RPE. It is interesting to note that both the NHP threshold data in the VIS range discussed in [3] and [4], as well as the data in the NIR range are consistent with effective laser spot sizes of 80–90 µm. When scattering is the underlying effect, one would expect a stronger effect in the VIS than in the NIR range. This could still be the case when the smaller extent of scattering in the NIR is compensated by the chromatic aberration effect that enlarges the spot in the NIR as compared to the VIS range. However, it still could be the case that also for the NHP experiment the laser spot diameter is smaller than 80–90 µm, because the observed injury threshold (lower than the computer model prediction for small laser spots) is also consistent with a small laser spot and a small lesion size at the RPE level (smaller than predicted by the computer model), when some biological amplification mechanism, potentially involving the photoreceptors or nerve fiber layers, makes the lesion detectable for visual observation of the fundus after 1 h or 24 h of exposure. This would still constitute a super-threshold lesion compared to the non-visible (at threshold) case (modeled by the 50 µm spot diameter and 30 µm MVL in Figure 3C), but to a lesser degree as predicted by the computer model. The authors still find the explanation of a larger laser spot size more consistent with all the data, as the NHP thresholds are consistent with an 80–90 µm spot size not only for thermally induced injury in the millisecond regime, but also for nanosecond pulses where micro-cavitation is the underlying damage mechanism. Both the nanosecond NHP data reported by Zuclich et al. [21] as well as 100 ms NHP data [22] (both for 532 nm laser radiation) show no spot size dependence for nominal spot sizes less than approximately 80–100 µm when plotted as relative IOE in Figure 5 – which would be somewhat peculiar in its consistency if the laser spot were smaller than 80 µm, as the different spot sizes would be associated with strongly varying radiant exposure levels, implying that the above mentioned amplification mechanism would have to also depend on spot size and/or radiant exposure. However, as long as smaller spot sizes cannot be ruled out for instance in the human case for the fovea, as has already been noted in [3, 4], the exposure limits for small spots cannot be adjusted by increasing the value of α_{min}.

4.3. Comparison with draft exposure limits

In addition to further support for the earlier conclusions regarding the injury mechanism and the small spot issue as discussed in the previous section, the data complement the threshold collection that is important to have available for comparison with proposals for improved exposure limits in the field of laser safety. A consistent set of thresholds which characterizes the spot size dependence for the full range of pulse durations – which is not available for the NHP model – is of critical importance for the validation of the proposed time dependent α_{max} for the update of the exposure limits. The threshold data of the NHP computer model, being a conservative model for exposure of the human retina, is plotted together with the proposed amended exposure limits in Figure 6A in terms of spot diameter dependence and in Figure 6B in terms of pulse duration dependence. The

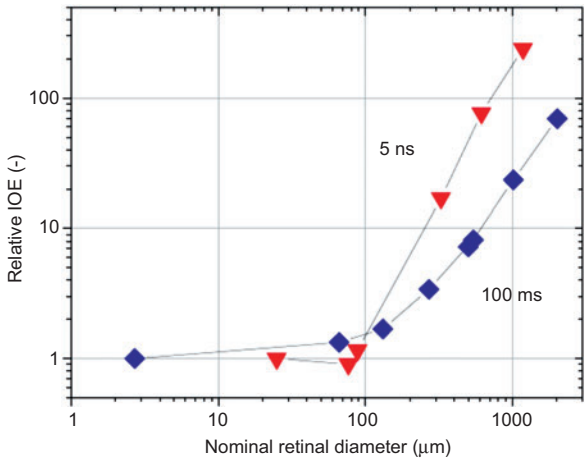

Figure 5 NHP thresholds (macular, 24 h endpoint) for two different pulse durations, plotted relative to the threshold of the smallest spot in the respective series; the 5 ns data is from Zuclich et al. [21] and the 100 ms data is from Lund et al. [22].

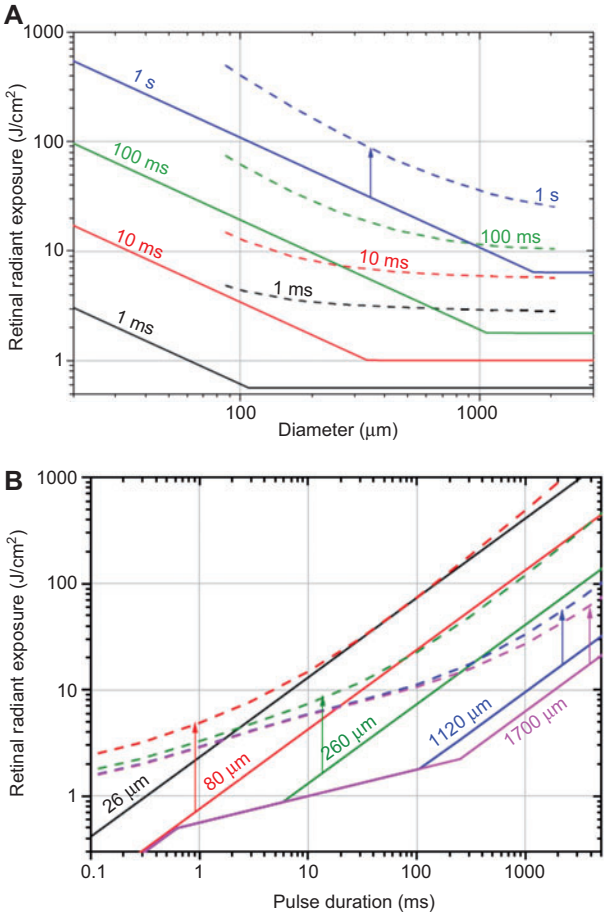

Figure 6 Comparison of the NHP computer model thresholds with the proposed laser exposure limits (A) as function of retinal spot size, and (B) as function of pulse duration. An ocular transmittance of 0.62 was used to obtain values as retinal radiant exposure. Small spot data is not shown as the NHP model (90 µm minimal spot size) predicts thresholds that might be too high for the human case, where a smaller minimal spot size cannot be ruled out.

pulse duration dependent α_{max} (in mrad), $\alpha_{max}=200\ t^{0.5}$ (t in seconds) was used to determine the exposure limits, where for the example of a pulse duration of 1 ms, $\alpha_{max}=6.3$ mrad, corresponding to a retinal diameter of 107 µm in an air-filled equivalent human eye with a distance between the retina and the principle plane of the ocular imaging system of 17 mm [2]. For pulse durations shorter than 625 µs, $\alpha_{max}=5$ mrad (retinal image diameter of 85 µm) and for pulse durations longer than 250 ms, $\alpha_{max}=100$ mrad, as in the current exposure limits (retinal image diameter of 1.7 mm). The pulse duration dependent α_{max} results in a pulse duration dependence of the exposure limits which for spot sizes larger than 85 µm (5 mrad) features a section with a $t^{0.25}$ dependence, and a section with $t^{0.75}$ and limits identical to the current ones for pulse durations beyond a critical value that depends on spot size. This critical time is found by solving the dependence of α_{max} for t, and equals 109 ms for the example of a retinal spot size of 1120 µm, one of our experimental spot diameters. The exposure limits were transformed into a retinal radiant exposure value by assuming a pre-retinal transmission factor of 62%. In terms of spot size dependence, the reduction factor (factor between threshold and exposure limit) is smallest in the region where the spot diameter dependence is about $1/D$, and somewhat larger in the region of large spots where there is no spot size dependence and also in the small spot region, where the thresholds exhibit a $1/D^2$ dependence but the exposure limit goes with $1/D$. In terms of pulse duration dependence, the reduction factor is larger for shorter pulses, as the pulse duration dependence of the threshold data becomes shallower at pulse durations where the exposure limit still features a $t^{0.75}$ dependence. However, it should be noted that for larger spots, the new pulse duration dependence of the exposure limits (being composed of a $t^{0.75}$ dependence for longer pulses and a $t^{0.25}$ dependence below the critical pulse duration) follows the injury thresholds much better than the current exposure limits and which continue to decrease with a $t^{0.75}$ dependence for pulse durations shorter than the critical one. The smallest reduction factors are found for the long pulse duration set (1 s); for the small spot case the smallest reduction factor is about 16, for extended sources about 5, found in the spot sizes range of 200–800 µm as marked with an arrow in Figure 6A.

These reduction factors are somewhat larger than the ones for the wavelength of 532 nm (which originates from the wavelength correction factor in the exposure limits which does not exactly follow the wavelength dependence of the threshold values), fully validating the proposed amendment of the exposure limits in the thermal injury regime for pulsed extended sources. Regarding the reduction factor for exposure durations of 1 s and longer, it is interesting to note that the NHP thresholds on the one hand, and the *ex-vivo* bovine and computer model thresholds on the other, do not deviate for pulse durations of 1 s thus confirming that blood flow, which is only present in the NHP *in-vivo* model, does not play a role in raising the injury thresholds, as already noted by Welsh et al. [23]. For exposure durations significantly longer than 1 s, blood flow as well as (for "awake" human) eye movements will raise the threshold values, thereby further increasing the reduction factors between injury threshold and exposure limit.

5. Conclusion

We report threshold data for thermally induced retinal injury for a wavelength of 1090 nm determined with an *ex-vivo* bovine and a computer model for the full applicable pulse duration and spot size range. This data set complements threshold values for 532 nm laser radiation from an earlier study. The data compare well with available NHP data and it can be concluded that the thermal damage computer model and the *ex-vivo* bovine model, for exposure durations between about 100 µs and several seconds, for all retinal spot sizes, are valid tools for the absolute prediction of NHP and human threshold levels also in the NIR range, up to a wavelength range of about 1340 nm. The proposed new international

exposure limits for pulsed and extended sources, introducing a pulse duration dependent α_{max}, are thereby confirmed for the complete applicable wavelength range.

The experimental and computer model data provide information pertaining to the basic understanding of laser bio-effects, as they are consistent with the assumption of a minimal spot size of 90 µm for the NHP model (a plausible explanation for the enlarged spot being pre-RPE scattering) and with the conclusion that scattering within the RPE and choroid does not play a significant role. Also the earlier conclusion, that for the NHP model, the underlying damage mechanism at thresholds detected 1 h or 24 h after exposure is immediate RPE cell damage, not thermal coagulation of the sensory retina, is supported.

Since the computer model was validated against *in-vivo* NHP data as well as *ex-vivo* bovine data in the VIS and the NIR wavelength range, in the future parameter studies and safety analysis can be conducted by application of the computer model for the applicable pulse duration and wavelength range. This is particularly relevant for irregular multiple pulses or scanned retinal exposure for which the current laser safety standards do not provide appropriate, or provide over restrictive evaluation methods.

Acknowledgments

We thank Letizia Farmer, Beate Fekete and Christine Höpfner from the Toxicology Department for obtaining bovine eyes from a slaughterhouse and preparation of the samples. We also thank Thomas Auzinger for programming the laser and scanner control software for the automated sample exposure.

References

[1] Sliney DH, Wolbarsht ML. Safety with lasers and other optical sources. New York: Plenum Press; 1980.

[2] Henderson R, Schulmeister K. Laser safety. Bristol and Philadelphia: Institute of Physics Publishing; 2004.

[3] Schulmeister K, Husinsky J, Seiser B, Edthofer F, Fekete B, Farmer L, Lund DJ. Ex vivo and computer model study on retinal thermal laser-induced damage in the visible wavelength range. J Biomed Opt 2008;13(5):054038.

[4] Schulmeister K, Stuck BE, Lund DJ, Sliney DH. Review of thresholds and exposure limits for laser and broadband optical radiation for thermally induced retinal injury. Health Phys 2011;100(2):210–20.

[5] International Commission on Non-Ionizing Radiation Protection (ICNIRP). Revision of guidelines on limits for laser radiation of wavelengths between 400 nm and 1.4 µm. Health Phys 2000;79(4):431–40. http://www.icnirp.de/documents/laser400nm+.pdf [Accessed 13 Feb 2012].

[6] Laser Institute of America. ANSI Z136.1-2007: American National Standard for Safe Use of Lasers. http://www.laserinstitute.org/store/product/106A [Accessed 13 Feb 2012].

[7] IEC 60825-1 – Ed. 2.0: 2007-03: Safety of laser products – Part 1: Equipment classification and requirements; equivalent European (German) standard: DIN EN 60825-1; VDE 0837-1:2008-05, Sicherheit von Lasereinrichtungen – Teil 1: Klassifizierung von Anlagen und Anforderungen, Deutsche Fassung EN 60825-1:2007.

[8] International Commission on Non-Ionizing Radiation Protection (ICNIRP). Guidelines on limits of exposure to broad-band incoherent optical radiation (0.38 to 3 µm). Health Phys 1997;73(3):539–54. http://www.icnirp.de/documents/broadband.pdf [Accessed 13 Feb 2012].

[9] International Commission on Illumination. CIE S009 (2002): Photobiological safety of lamps and lamp systems. http://www.cie.co.at/Publications/index.php?i_ca_id=474 [Accessed 13 Feb 2012].

[10] IEC 62471:2006: Photobiological safety of lamps and lamp systems; equivalent European (German) standard: DIN EN 62471 (VDE 0837-471), Photobiologische Sicherheit von Lampen und Lampensystemen, Deutsche Fassung EN 62471:2008.

[11] Schulmeister K. Expected changes for the retinal thermal exposure limits for broadband incoherent radiation of IEC 62471 and ICNIRP. Proceedings ILSC 2011, LIA, Orlando; 2011.

[12] Sliney DH, Mellerio J, Gabel VP, Schulmeister K. What is the meaning of threshold in laser injury experiments? Implications for human exposure limits. Health Phys 2002;82(3):335–47.

[13] Jean M, Schulmeister K. Laser-induced thermal damage of the rhesus monkey retina: computer model validation. Seibersdorf Laboratories Report L-LE-010/10, Seibersdorf; 2010.

[14] Takata AN, Goldfinch L, Hinds JK, Kuan LP, Thomopoulis N, Weigandt A. Thermal model of laser-induced eye damage. IIT Research Institute Report for Aerospace Medical Division, Chicago, IL; 1974.

[15] Welch AJ, Polhamus GD. Measurement and prediction of thermal injury to the retina of the rhesus monkey. IEEE Trans Biomed Eng 1984;31(10):633–43.

[16] Vincelette RL, Rockwell BA, Oliver JW, Kumru SS, Thomas RJ, Schuster KJ, Noojin GD, Shingledecker AD, Stolarski DJ, Welch AJ. Trends in retinal damage thresholds from 100-millisecond near-infrared laser radiation exposures: a study at 1,110, 1,130, 1,150, and 1,319 nm. Lasers Surg Med 2009;41(5):382–90.

[17] Ham Jr WT, Mueller HA, Ruffolo Jr JJ, Clarke AM. Sensitivity of the retina to radiation damage as a function of wavelength. Photochem Photobiol 1979;29(4):735–43.

[18] Skeen CH, Bruce WR, Tips JH, Smith MG, Garza GG. Ocular effects of near infrared laser radiation for safety criteria. USAFSAM, Report, Air Force Contract F41609-71-C-0016; 1972.

[19] Vassiliadis A, Rosan RC, Zweng HC. Research on ocular laser thresholds. Report SRI Project 7191, USAF School of Aerospace Medicine Contract F41609-68-C-0041; 1969.

[20] Maher EF. Transmission and absorption coefficients for ocular media of the rhesus monkey. USAF School of Aerospace Medicine Report SAM-TR-78-32, Brooks AFB, TX; 1978.

[21] Zuclich JA, Edsall PR, Lund DJ, Stuck BE, Hollins RC, Till S, Smith PA, McLin LN, Kennedy PK. Variation of laser-induced retinal damage threshold with retinal image size. J Laser Appl 2000;12(2):74–80.

[22] Lund DJ, Edsall P, Stuck BE, Schulmeister K. Variation of laser-induced retinal injury thresholds with retinal irradiated area: 0.1-s duration, 514-nm exposures. J Biomed Opt 2007;12(2):024023.

[23] Welsh AJ, Wissler EH, Priebe LA. Significance of blood flow in calculations of temperature in laser irradiated tissue. IEEE Trans Biomed Eng 1980;27(3):164–6.

Received January 8, 2012; revised February 22, 2012; accepted March 9, 2012